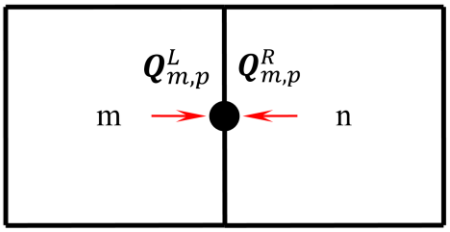

Figure 1 An example of flux calculation for finite volume method

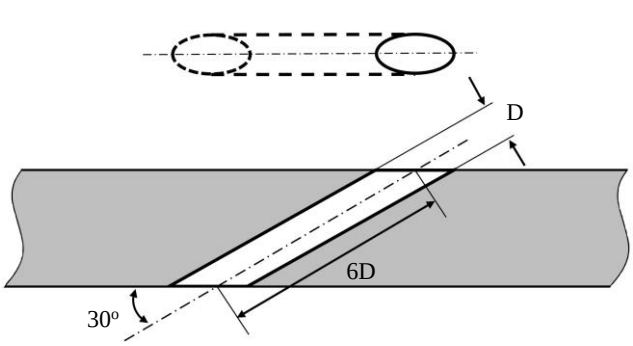

(a) Cylindrical hole

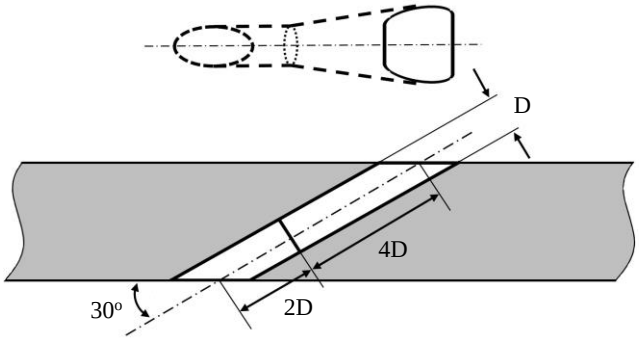

(b) Fan-shaped hole

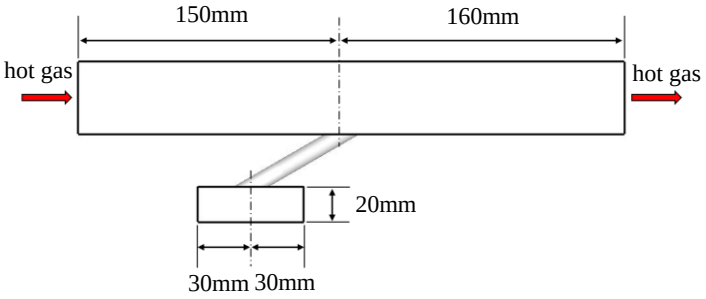

(c) Side view of the computational domain

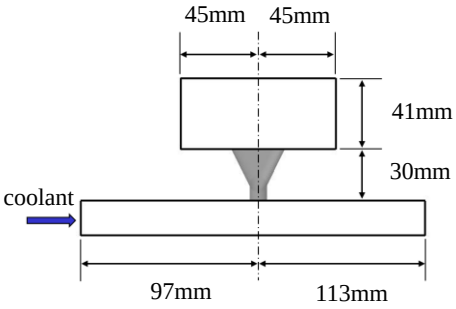

(d) Front view of the domain with fan-shaped hole

Figure 2 Hole geometry and computational domain of a typical flat plate film cooling model

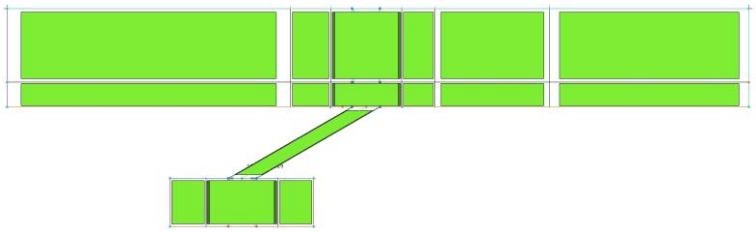

(a) Side view

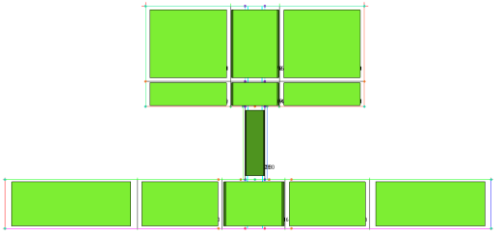

(b) Front view

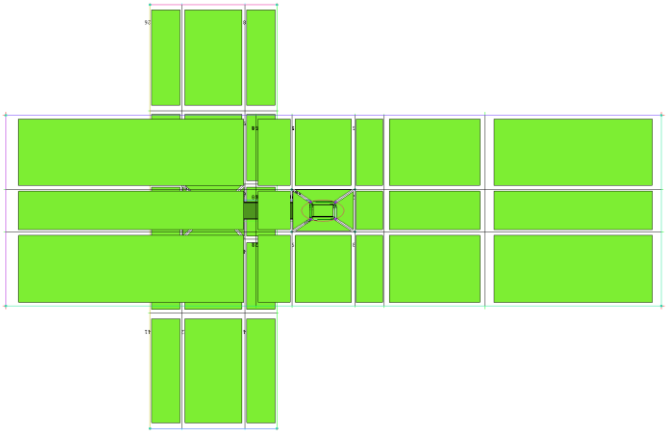

(c) Top view

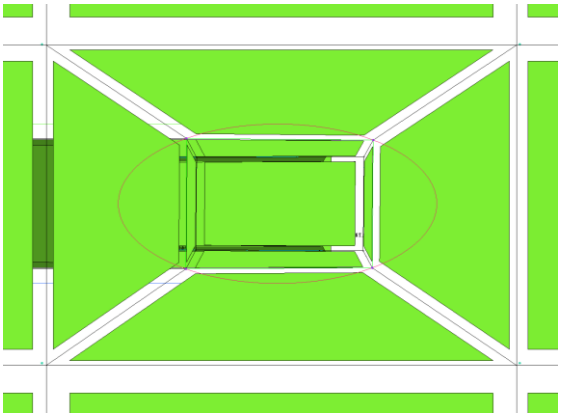

(d) Close-up of O-Type for hole

Figure 3 A unified multi-block layout for mesh generations

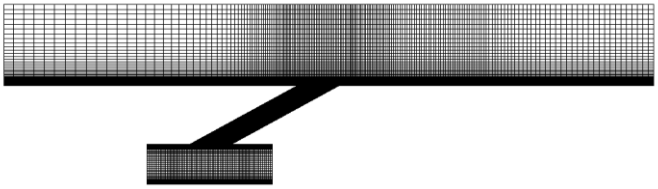

(a) Side view

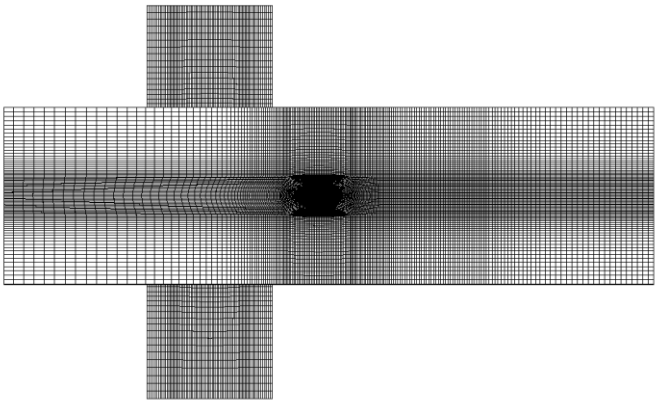

(b) Top view

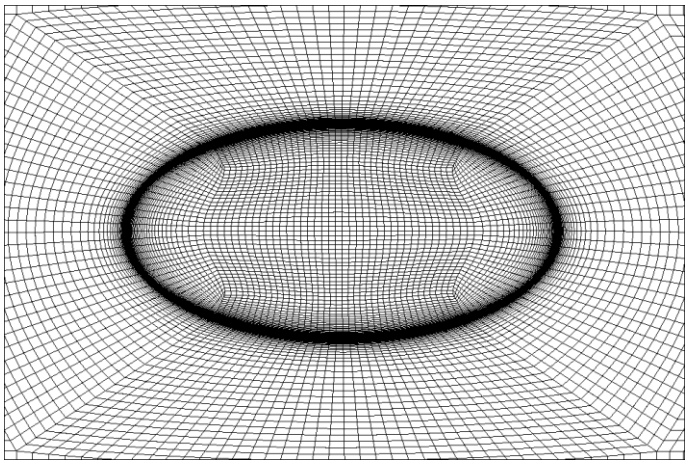

(c) Close-up for cylindrical hole

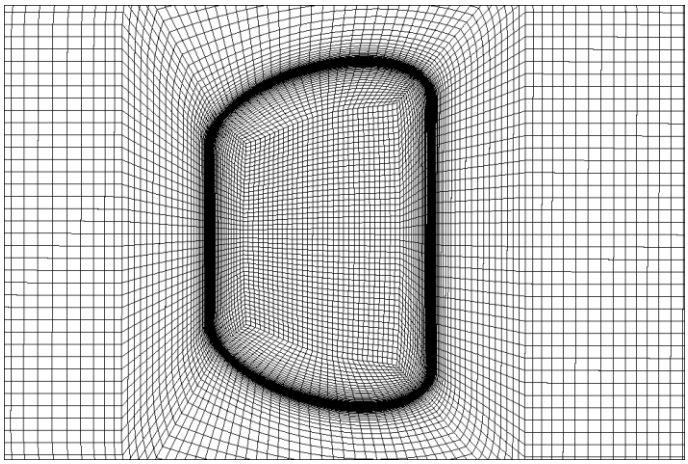

(d) Close-up for fan-shaped hole

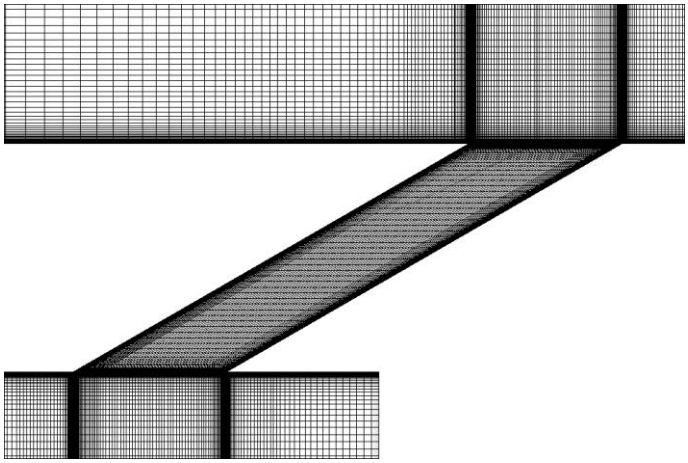

(e) Mid slice of volume mesh

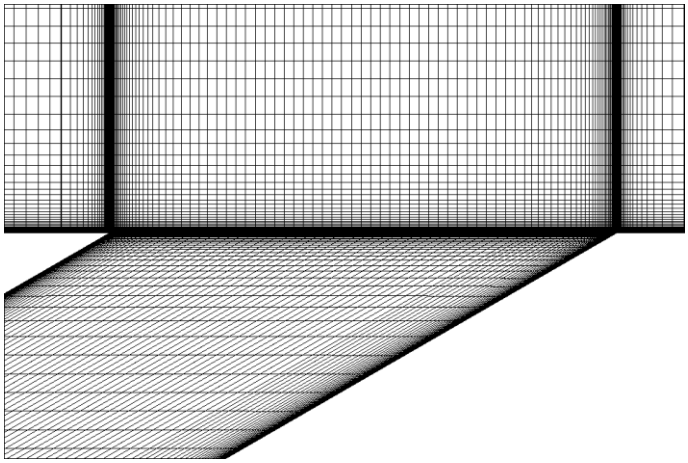

(f) Close-up for hole exit

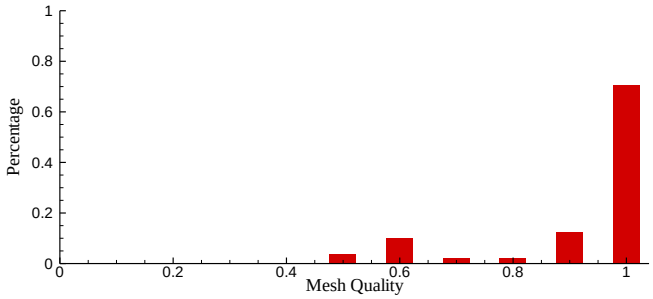

(g) Mesh quality of cylindrical hole

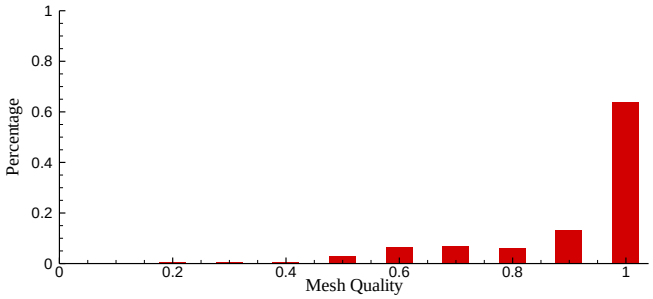

(h) Mesh quality of fan-shaped hole

Figure 4 Details of the fine mesh generated for the film cooling flow simulations

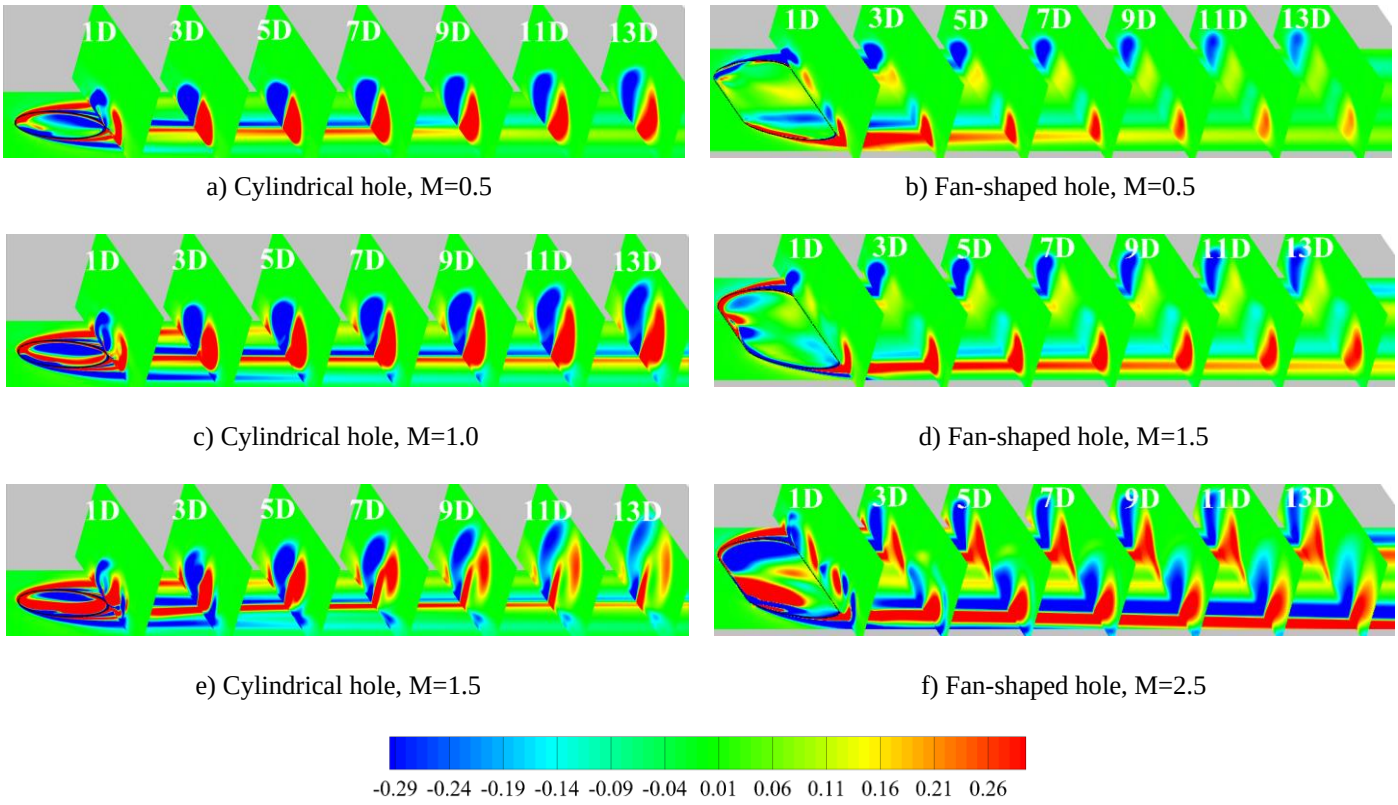

a) Cylindrical hole, M=0.5 b) Fan-shaped hole, M=0.5

c) Cylindrical hole, M=1.0 d) Fan-shaped hole, M=1.5

e) Cylindrical hole, M=1.5 f) Fan-shaped hole, M=2.5

Figure 5 Contour of the non-dimensional normal-component vorticity solved by the respective fine meshes

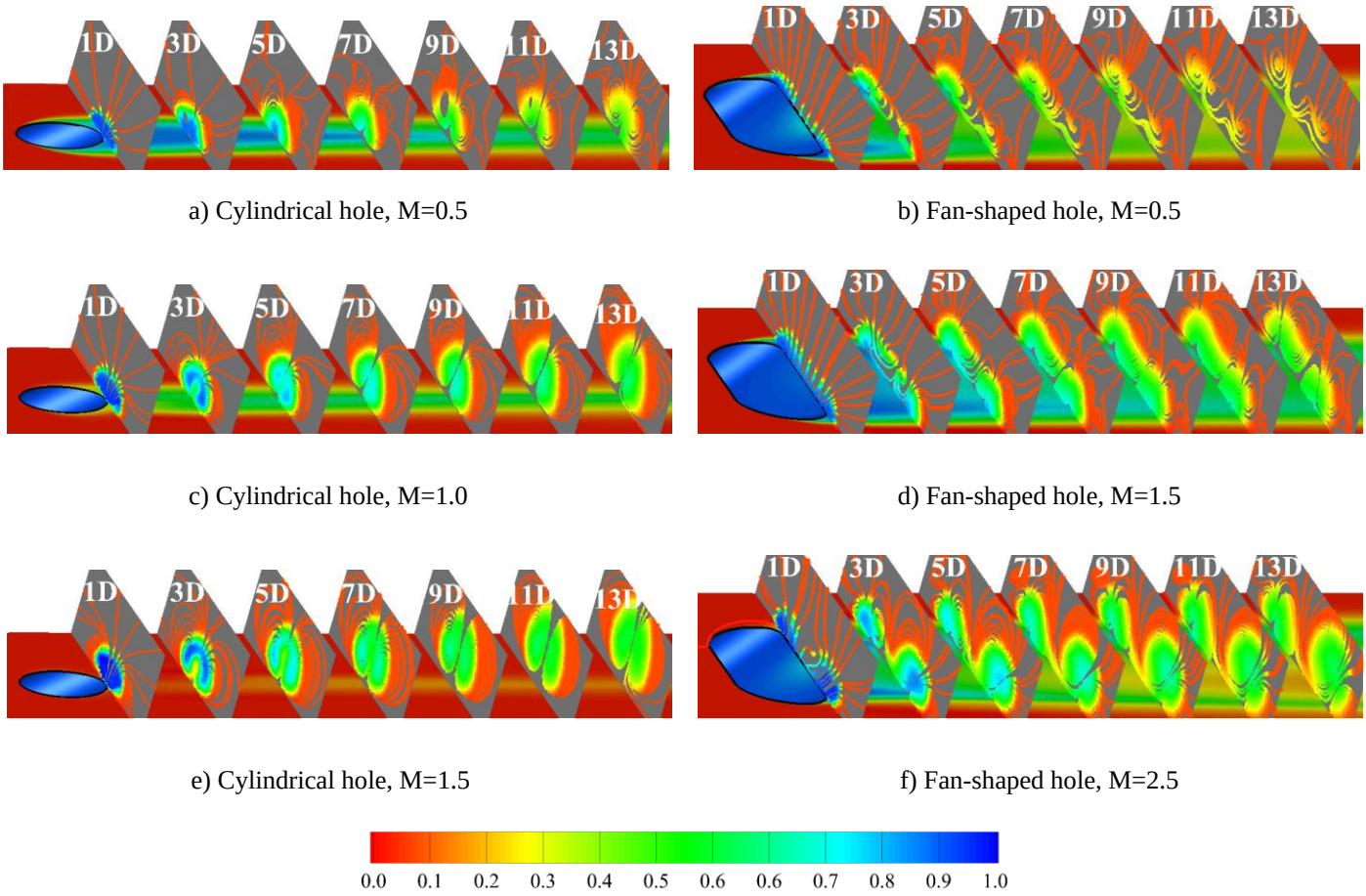

a) Cylindrical hole, M=0.5 b) Fan-shaped hole, M=0.5

c) Cylindrical hole, M=1.0 d) Fan-shaped hole, M=1.5

e) Cylindrical hole, M=1.5 f) Fan-shaped hole, M=2.5

Figure 6 Non-dimensional temperature field with streamlines at different slices (fine mesh)

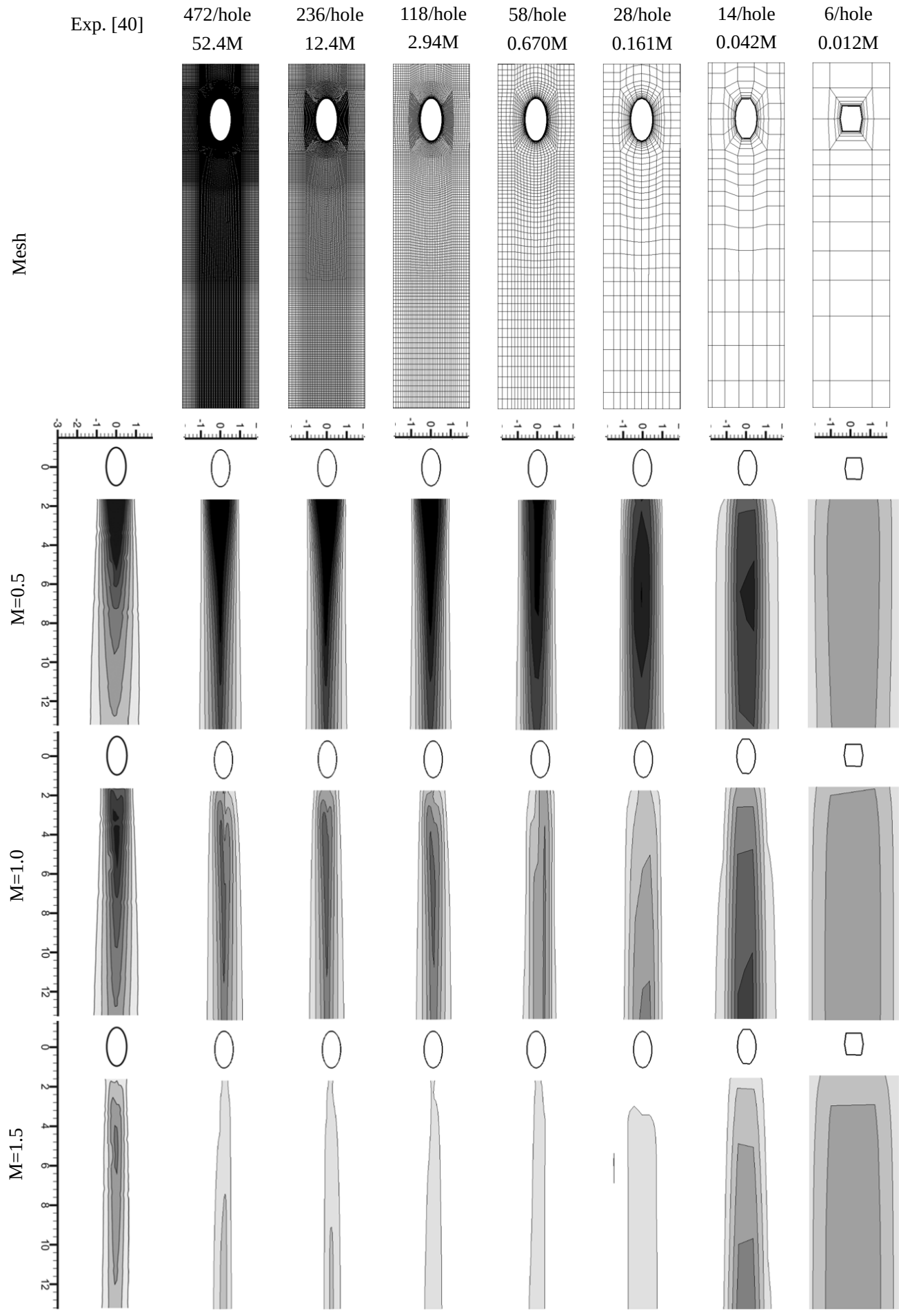

Figure 7 Mesh sensitivity of film effectiveness for cylindrical hole

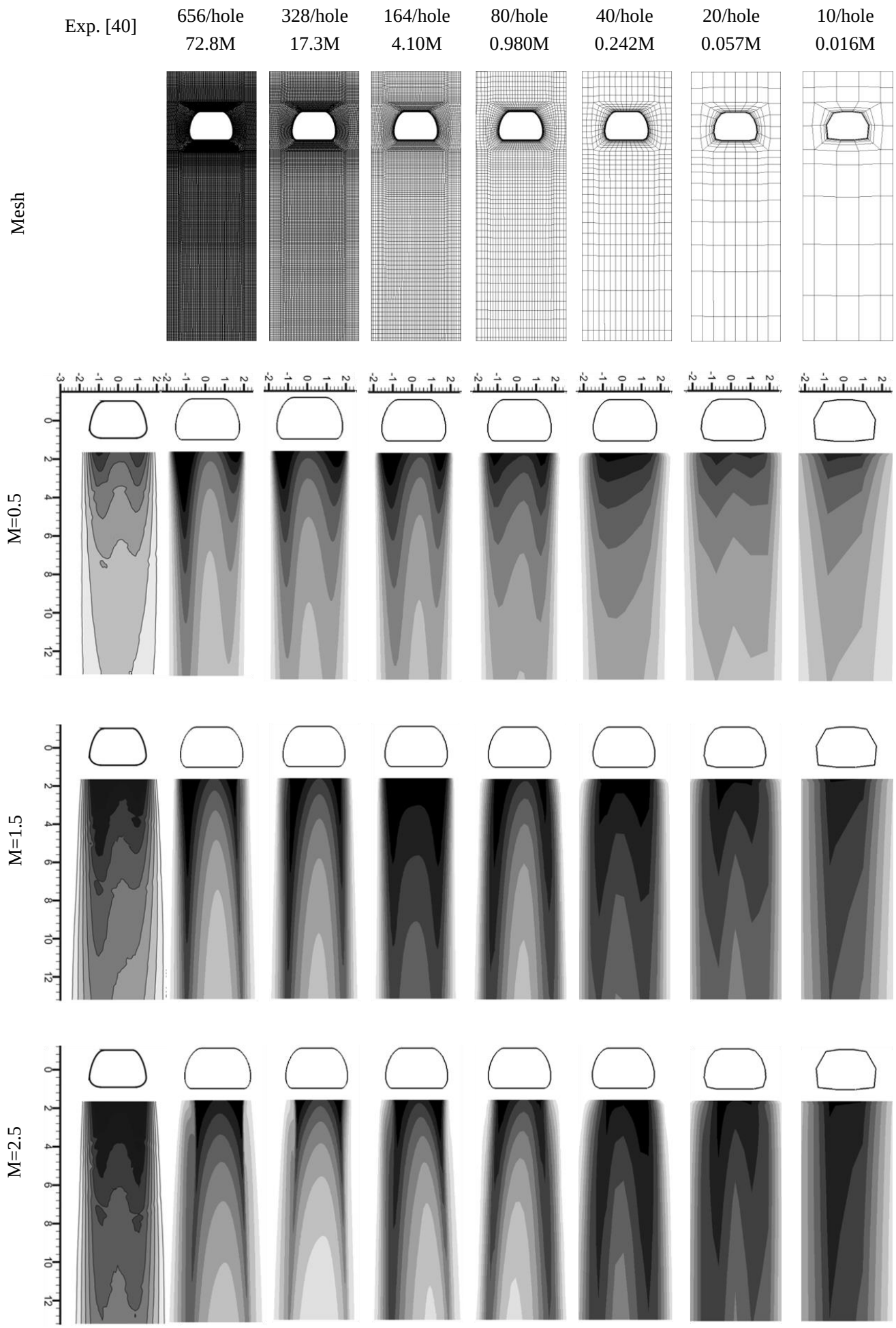

Figure 8 Mesh sensitivity of film effectiveness for fan-shaped hole

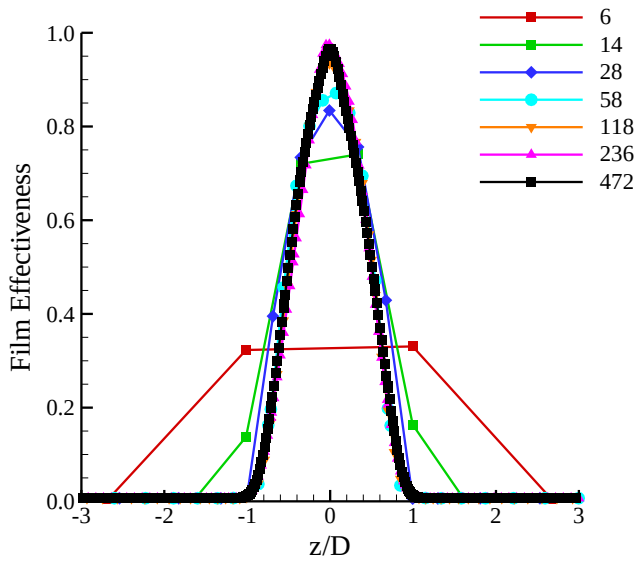

a) Cylindrical hole, M=0.5

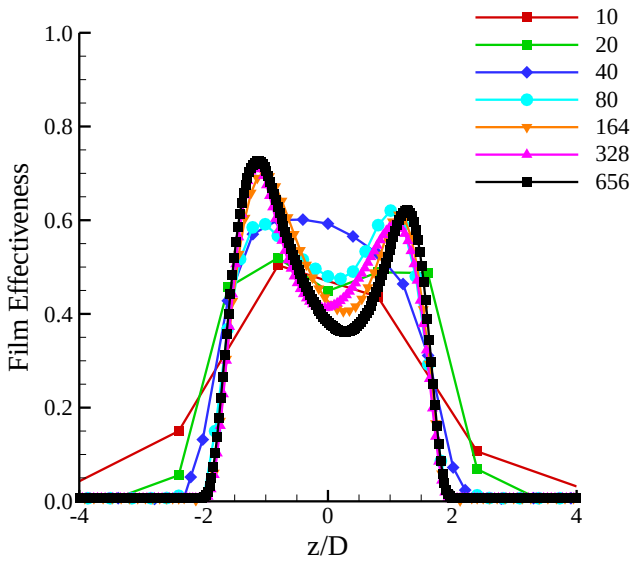

b) Fan-shaped hole, M=0.5

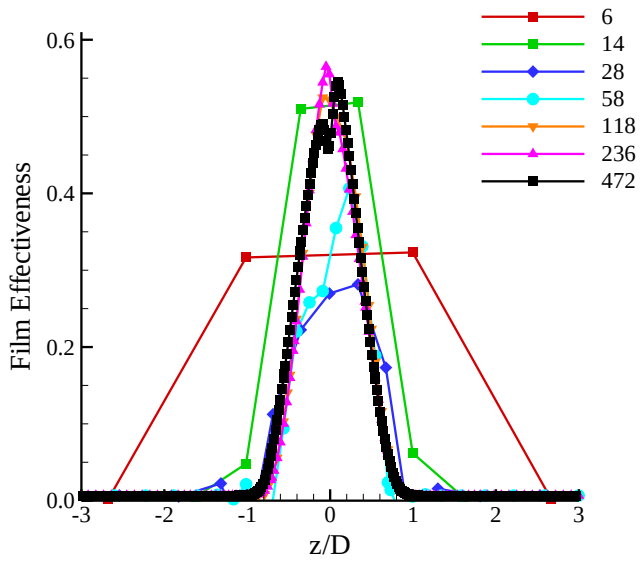

c) Cylindrical hole, M=1.0

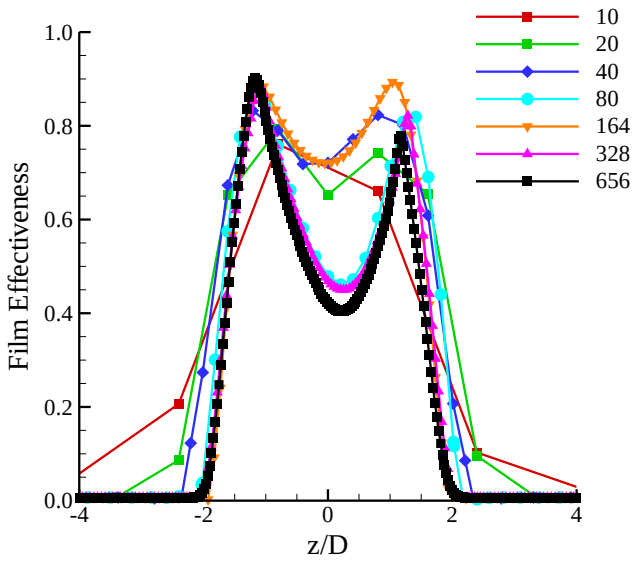

d) Fan-shaped hole, M=1.5

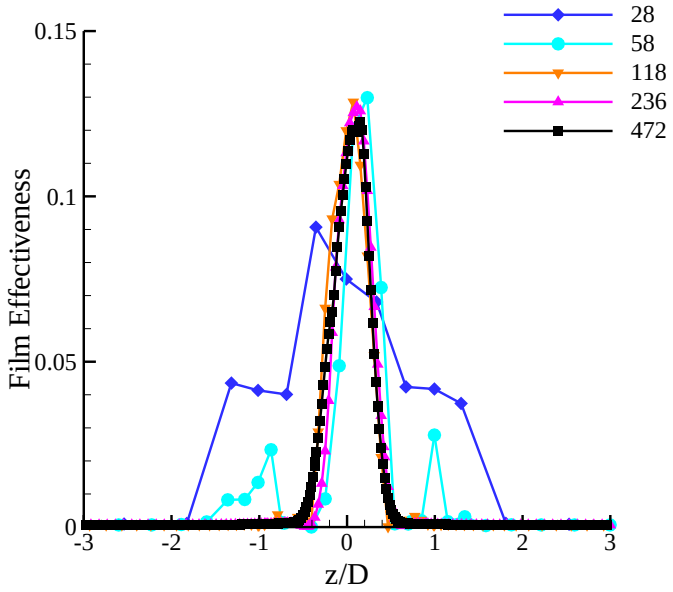

e) Cylindrical hole, M=1.5

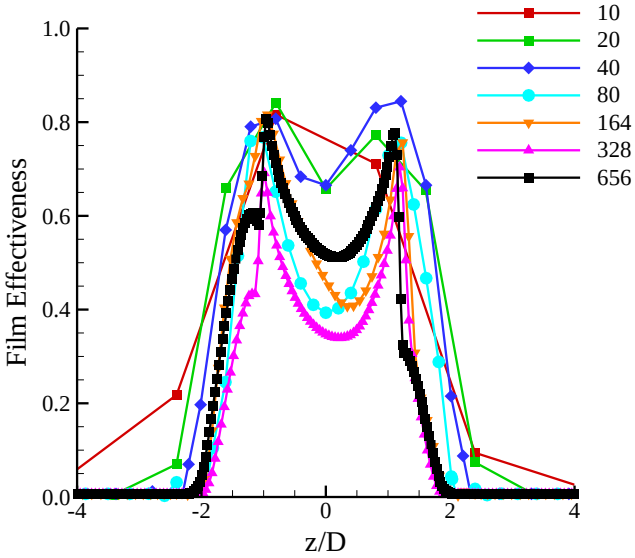

f) Fan-shaped hole, M=2.5

Figure 9 Mesh sensitivity of lateral film effectiveness at x/D=5 downstream

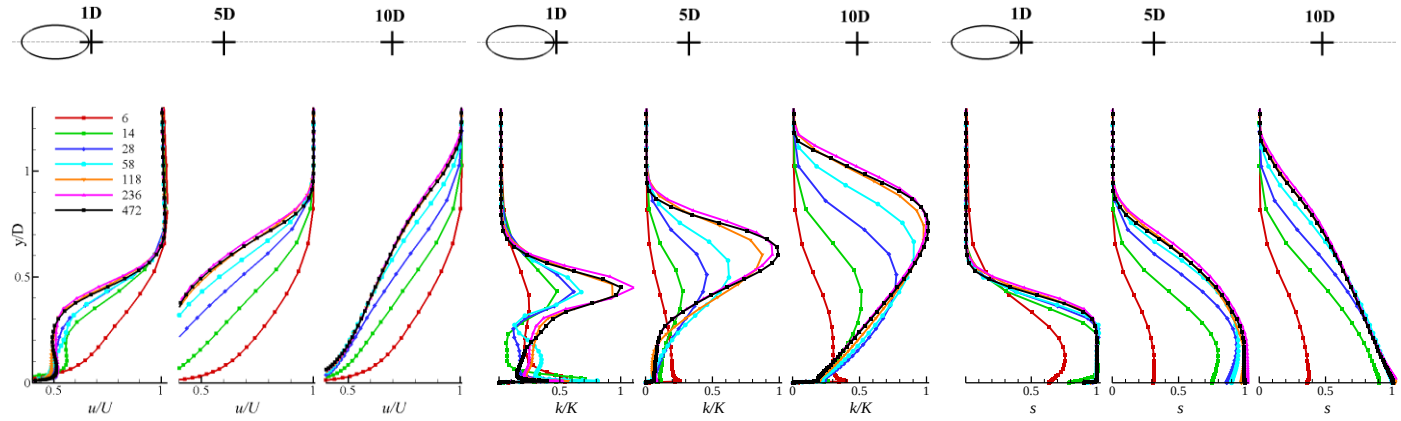

a) M=0.5

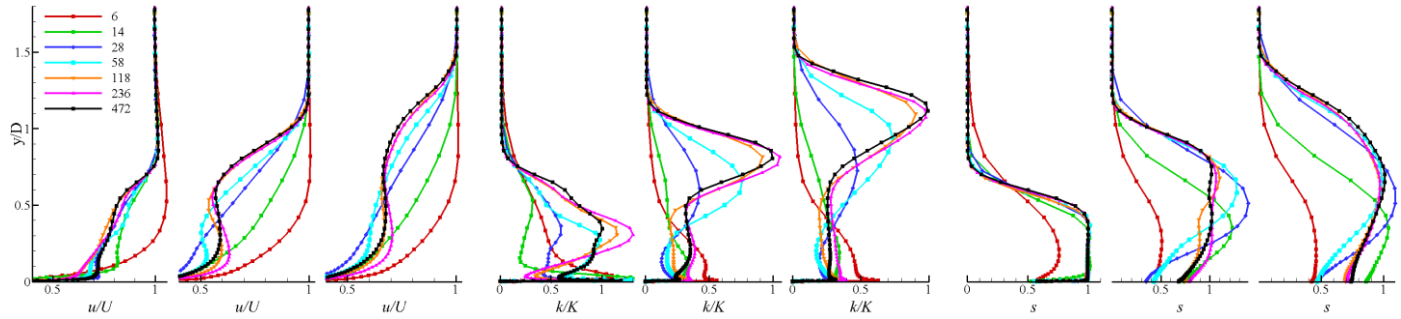

b) M=1.0

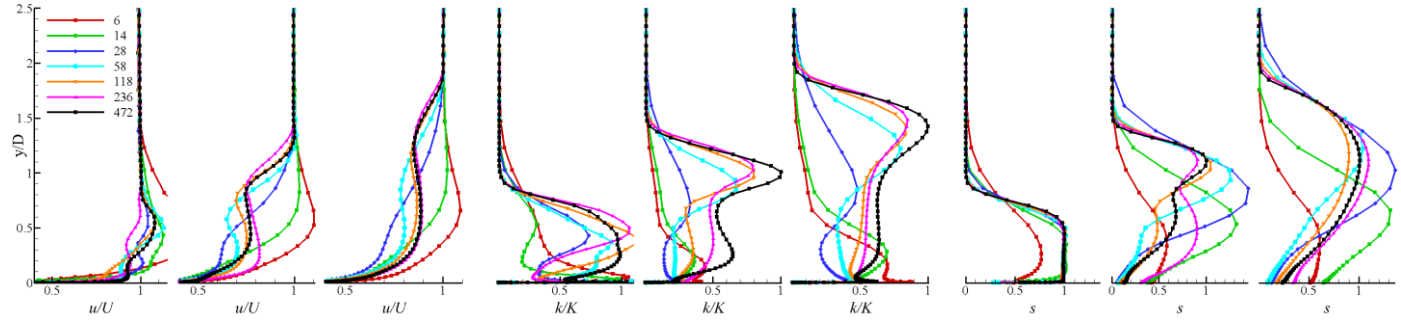

c) M=1.5

Figure 10 Mesh sensitivity of boundary layer profiles

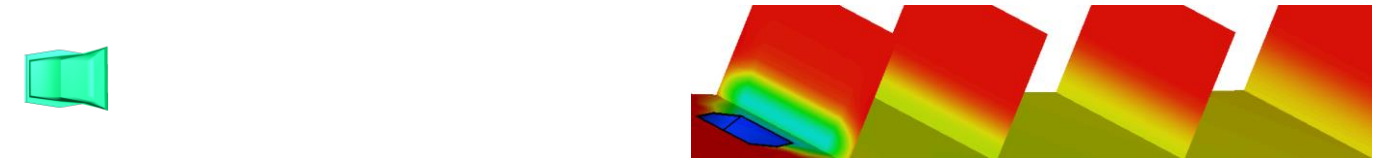

a) 0.012M mesh nodes with 6 nodes around the hole

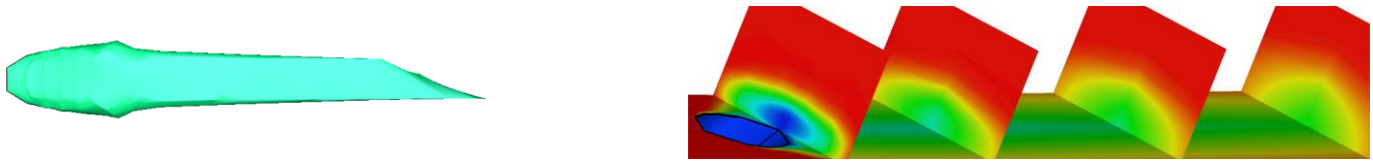

b) 0.042M mesh nodes with 14 nodes around the hole

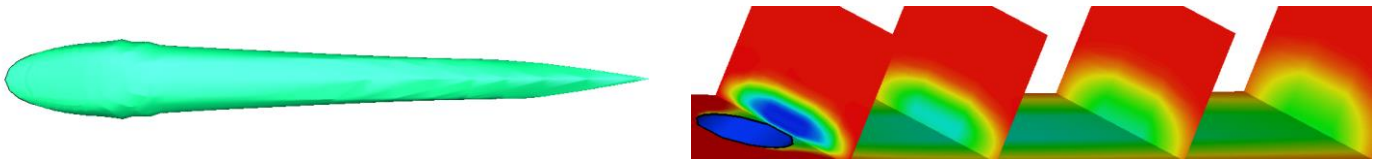

c) 0.161M mesh nodes with 28 nodes around the hole

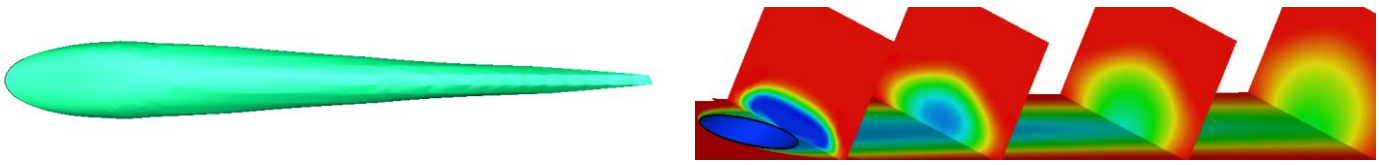

d) 0.670M mesh nodes with 58 nodes around the hole

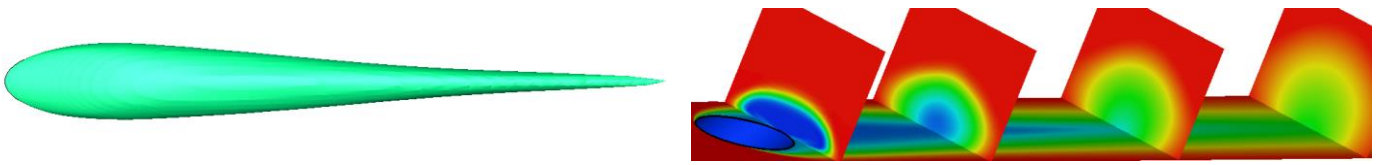

e) 2.94M mesh nodes with 118 nodes around the hole

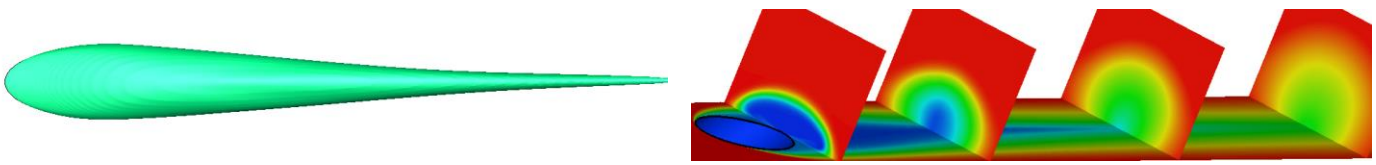

f) 12.4M mesh nodes with 236 nodes around the hole

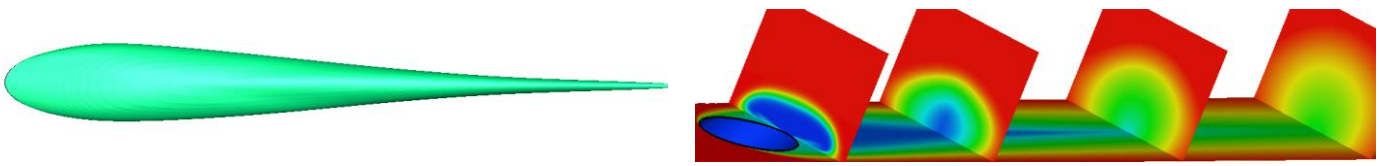

g) 52.4M mesh nodes with 472 nodes around the hole

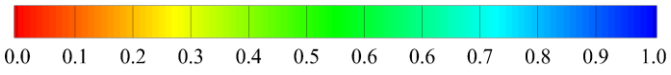

Figure 11 Mesh sensitivity of iso-surface and slices of temperature defect on the cylindrical hole, blowing ratio 0.5

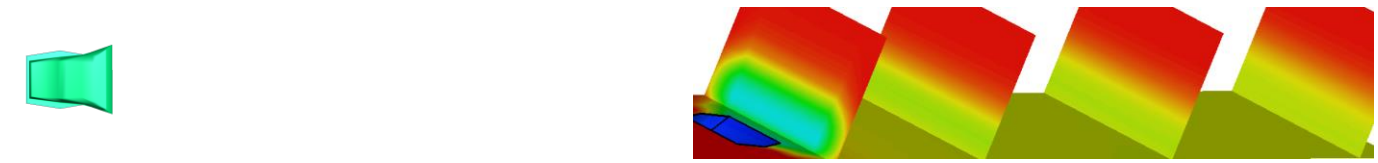

a) 0.012M mesh nodes with 6 nodes around the hole

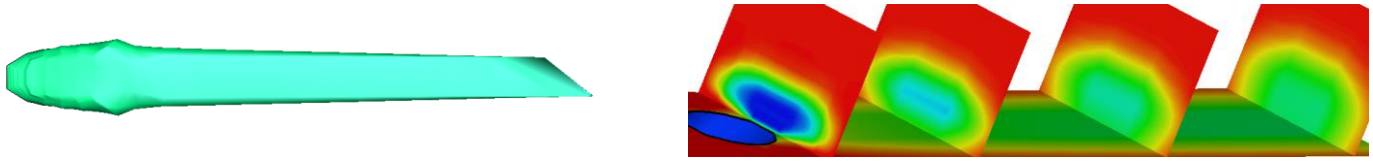

b) 0.042M mesh nodes with 14 nodes around the hole

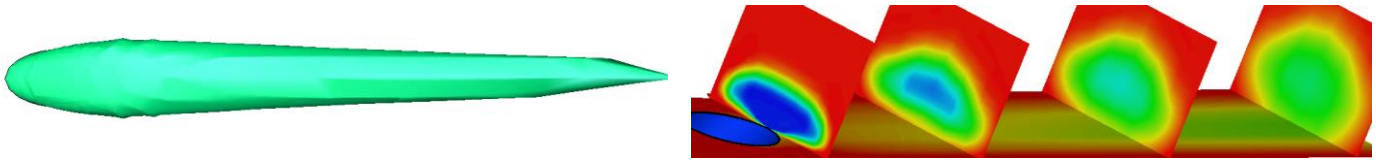

c) 0.161M mesh nodes with 28 nodes around the hole

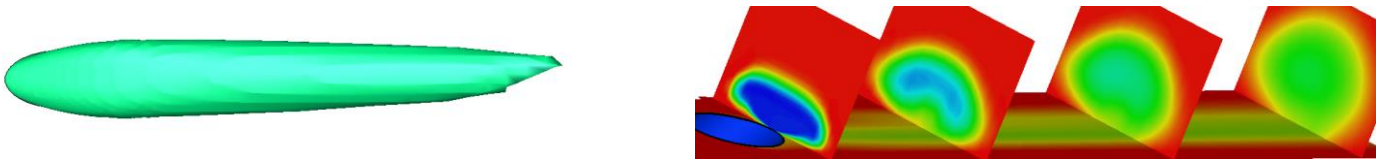

d) 0.670M mesh nodes with 58 nodes around the hole

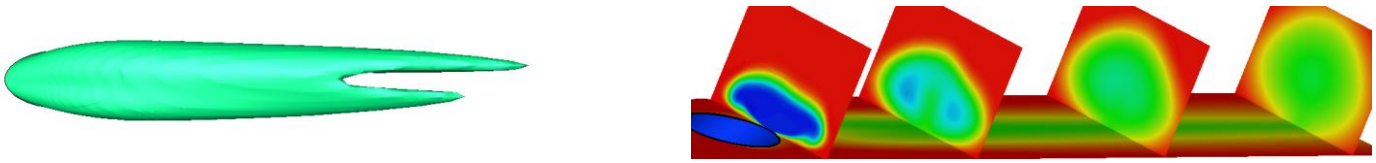

e) 2.94M mesh nodes with 118 nodes around the hole

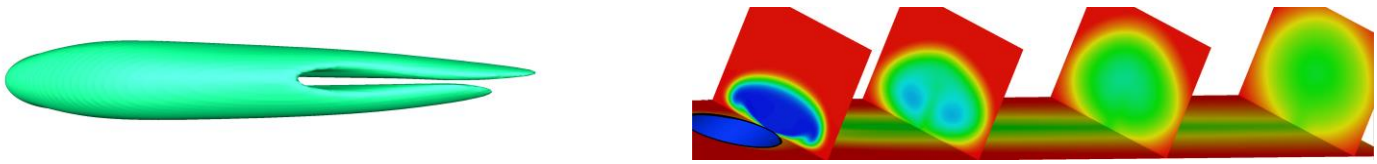

f) 12.4M mesh nodes with 236 nodes around the hole

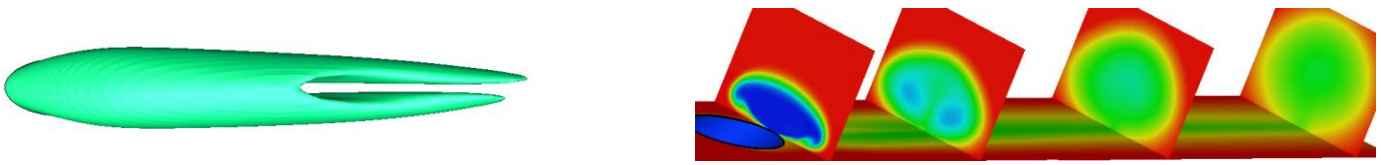

g) 52.4M mesh nodes with 472 nodes around the hole

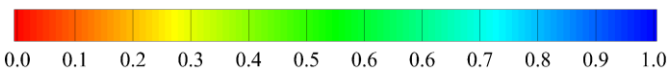

Figure 12 Mesh sensitivity of iso-surface and slices of temperature defect on the cylindrical hole, blowing ratio 1.0

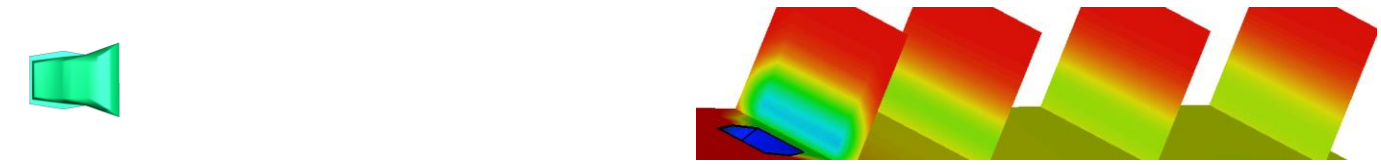

a) 0.012M mesh nodes with 6 nodes around the hole

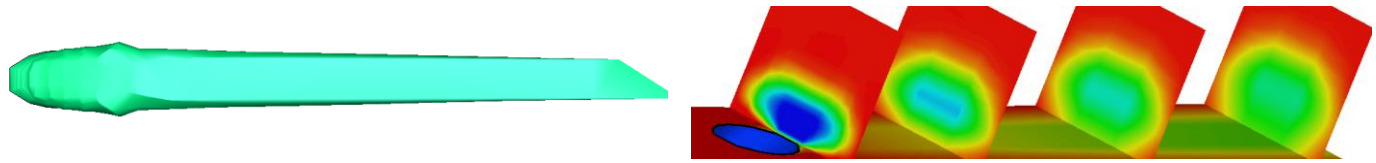

b) 0.042M mesh nodes with 14 nodes around the hole

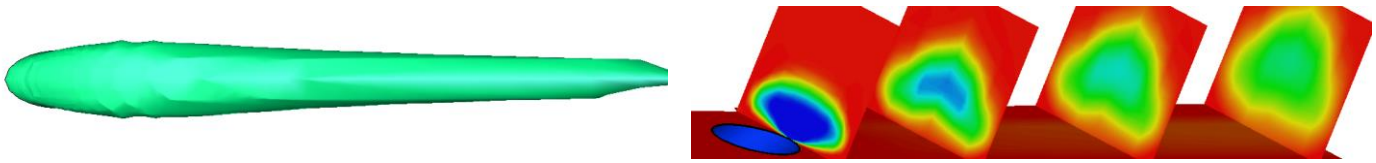

c) 0.161M mesh nodes with 28 nodes around the hole

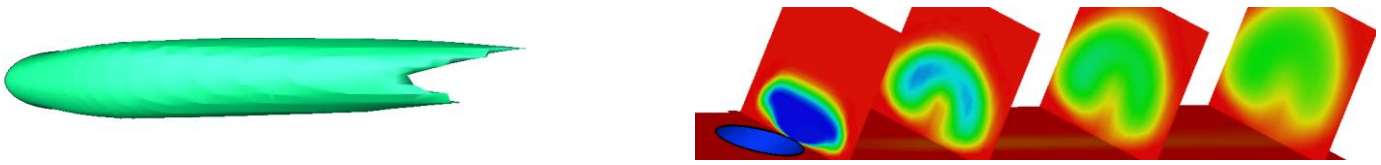

d) 0.670M mesh nodes with 58 nodes around the hole

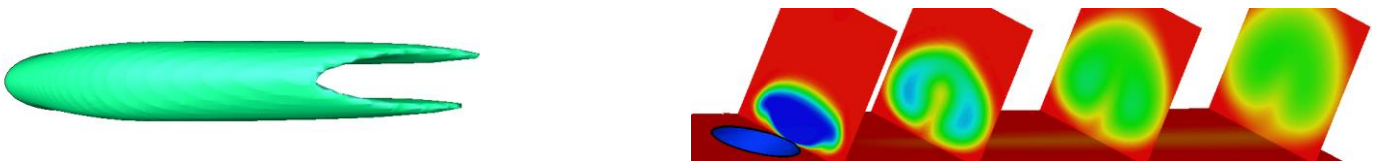

e) 2.94M mesh nodes with 118 nodes around the hole

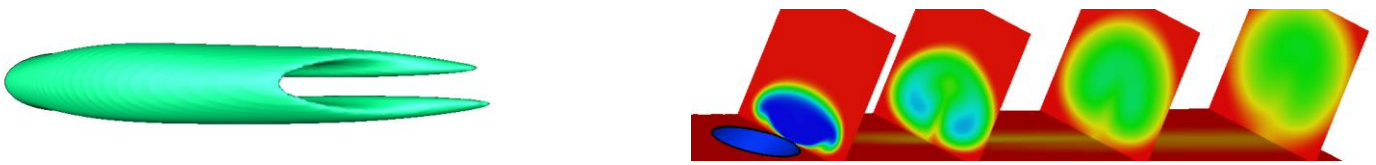

f) 12.4M mesh nodes with 236 nodes around the hole

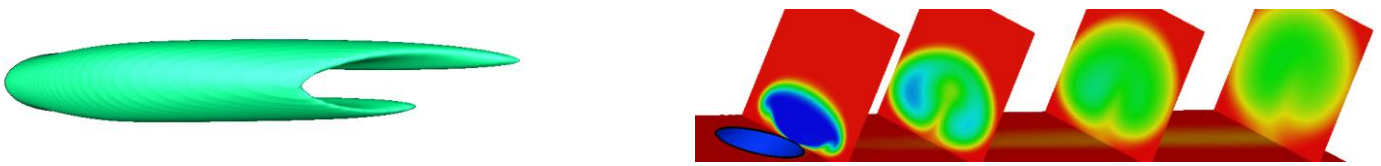

g) 52.4M mesh nodes with 472 nodes around the hole

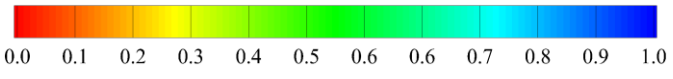

Figure 13 Mesh sensitivity of iso-surface and slices of temperature defect on the cylindrical hole, blowing ratio 1.5

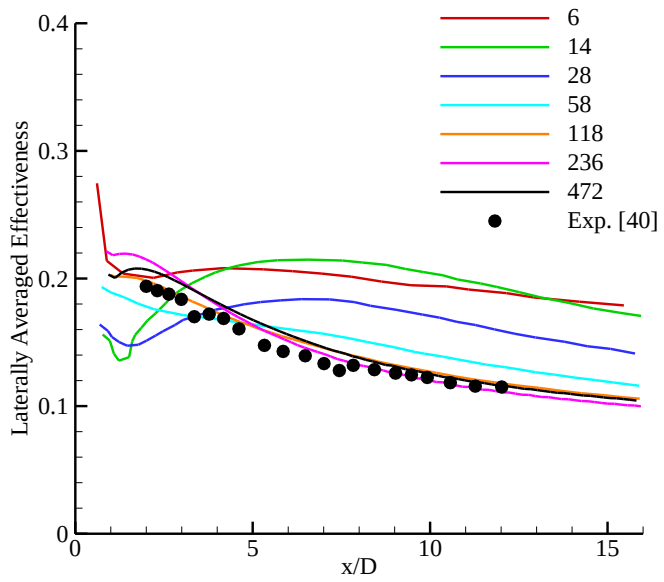

a) Cylindrical hole, M=0.5

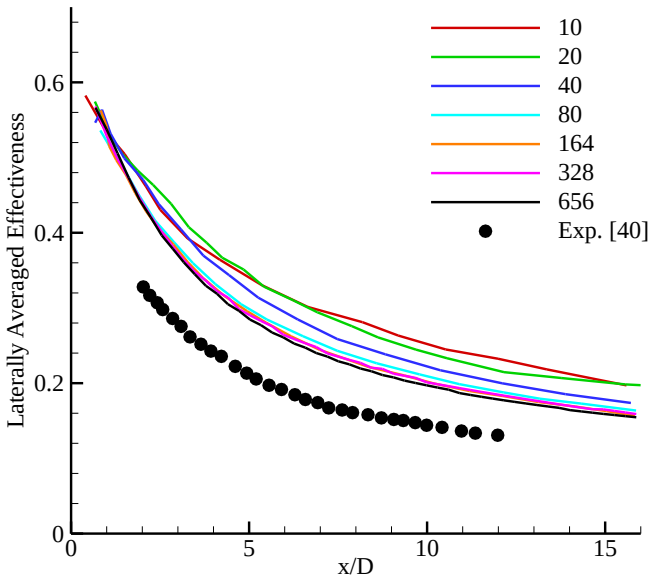

b) Fan-shaped hole, M=0.5

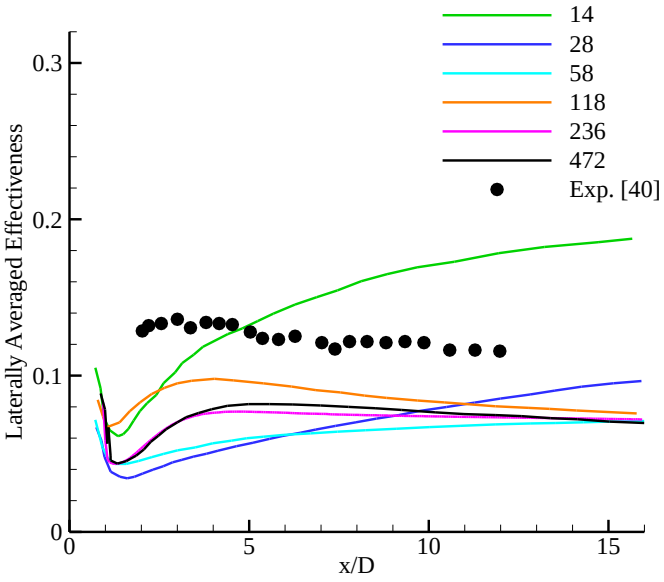

c) Cylindrical hole, M=1.0

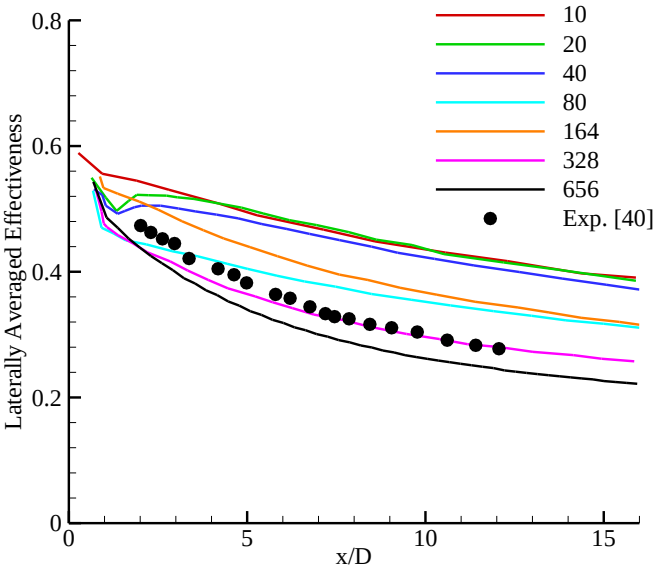

d) Fan-shaped hole, M=1.5

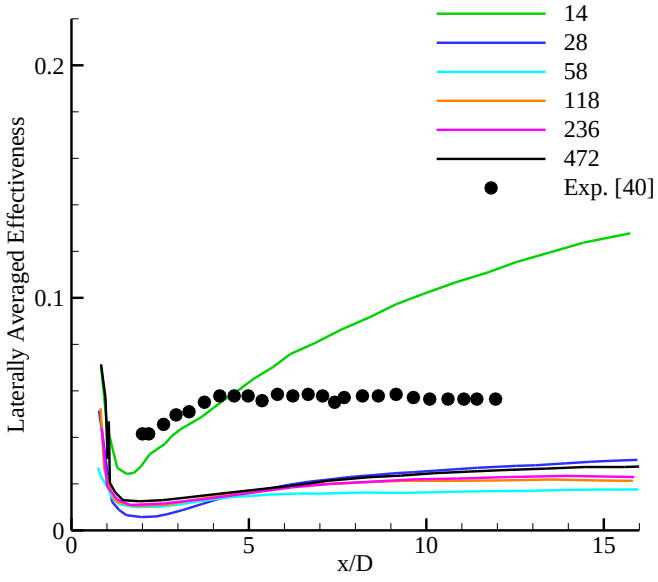

e) Cylindrical hole, M=1.5

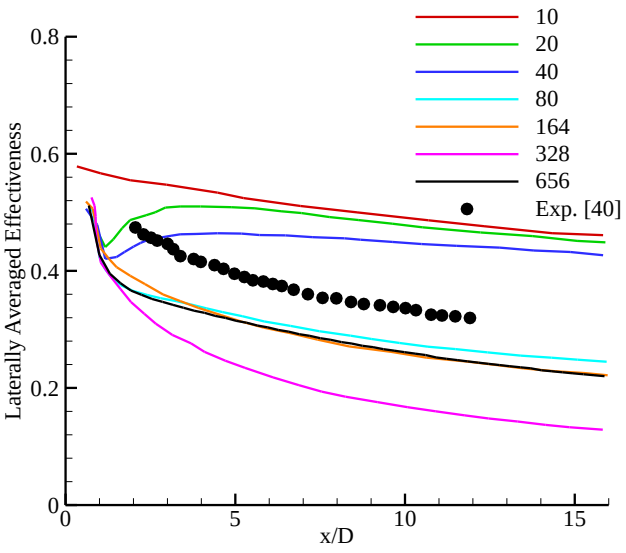

f) Fan-shaped hole, M=2.5

Figure 14 Mesh sensitivity of laterally averaged film effectiveness

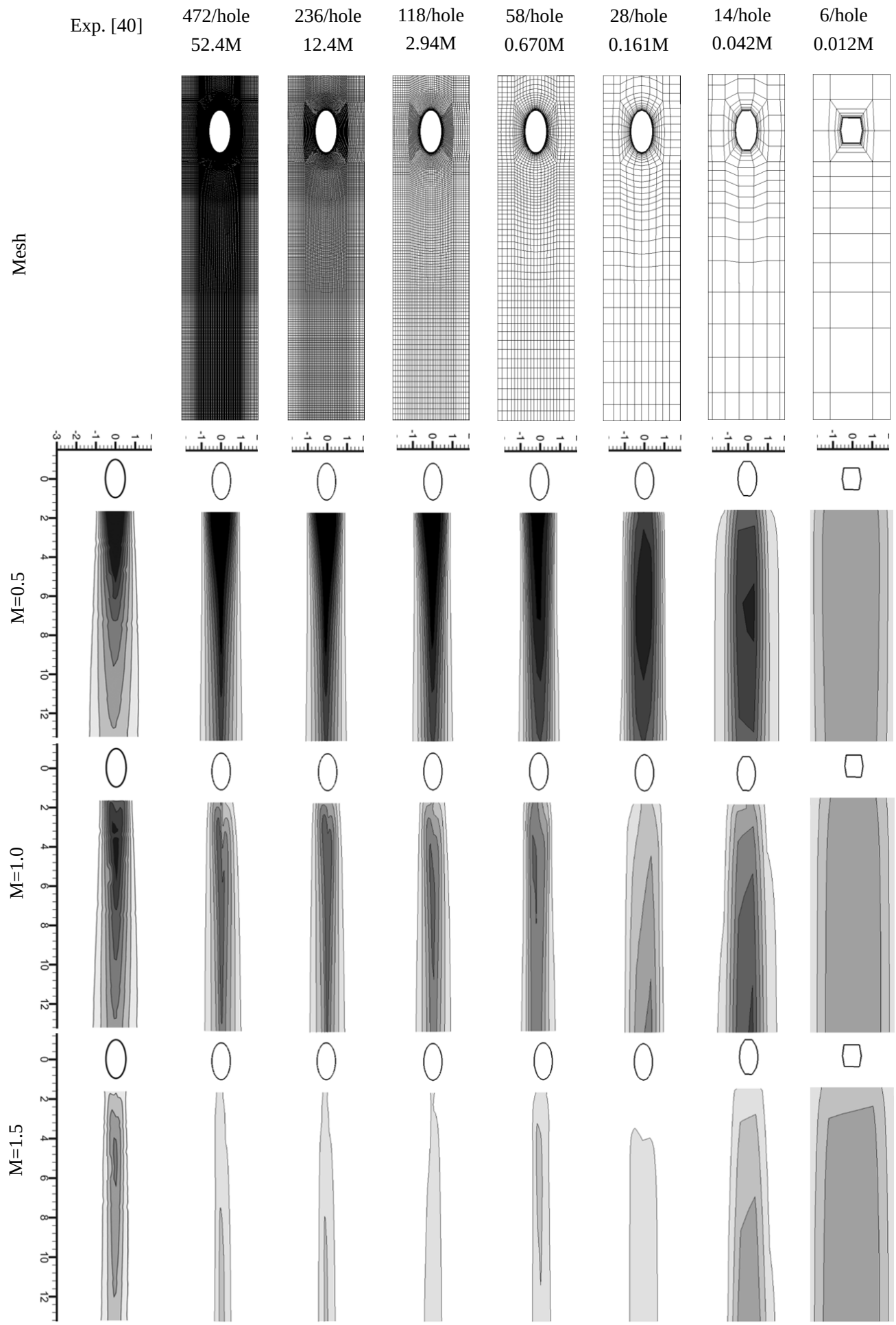

Figure A1 Mesh sensitiveness of film effectiveness with a fixed wall-normal nodes spacing

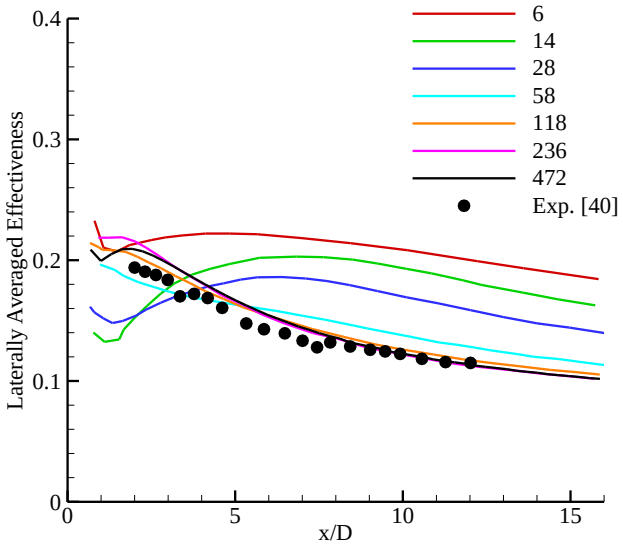

a) Cylindrical hole, M=0.5

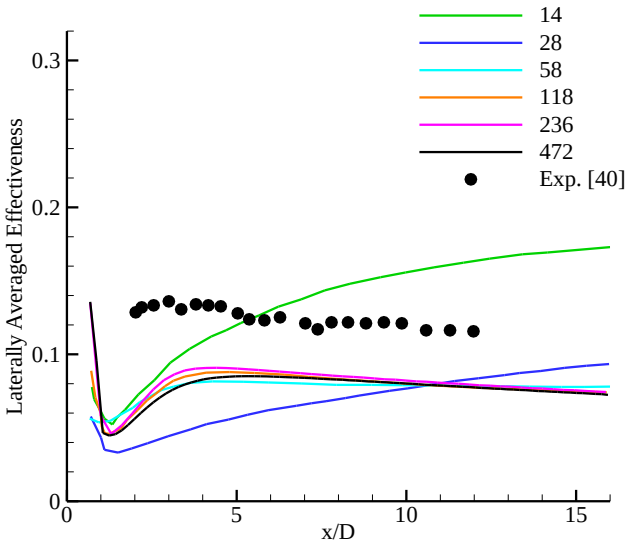

b) Cylindrical hole, M=1.0

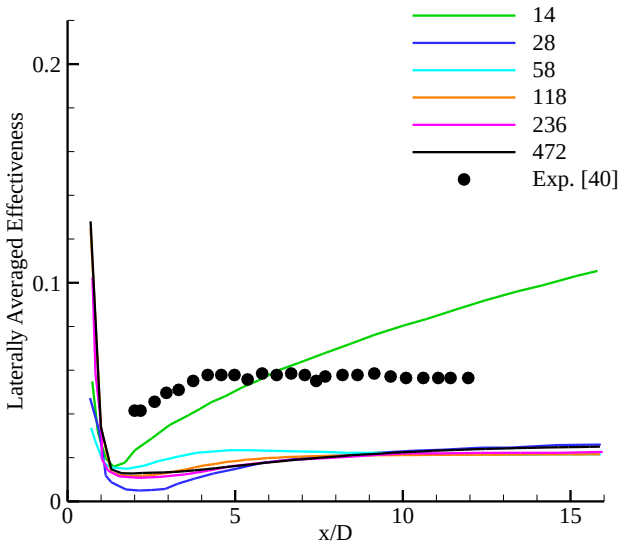

c) Cylindrical hole, M=1.5

Figure A2 Mesh sensitivity of laterally averaged film effectiveness with a fixed wall-normal nodes spacing

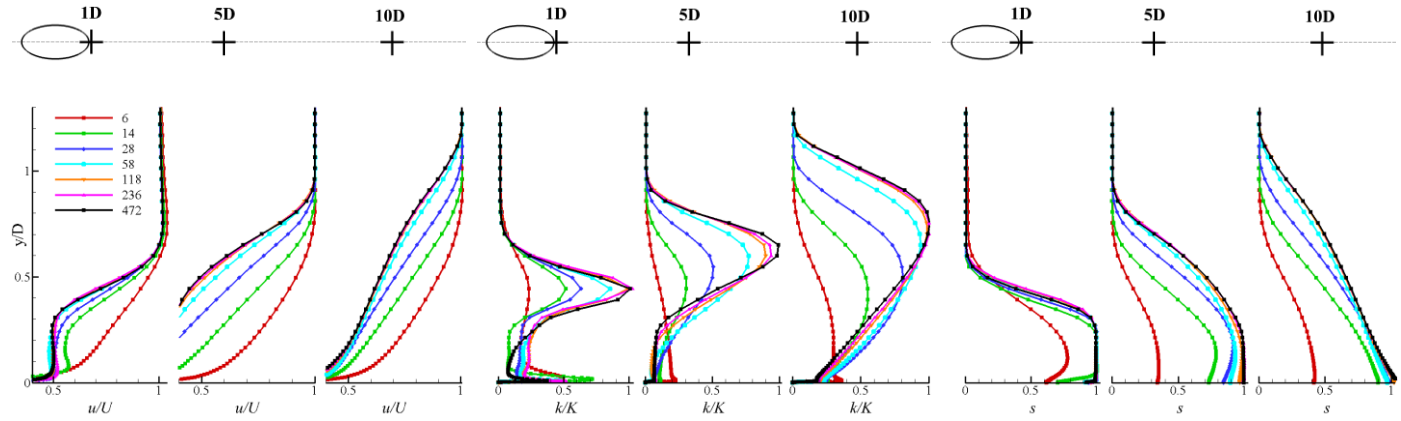

a) M=0.5

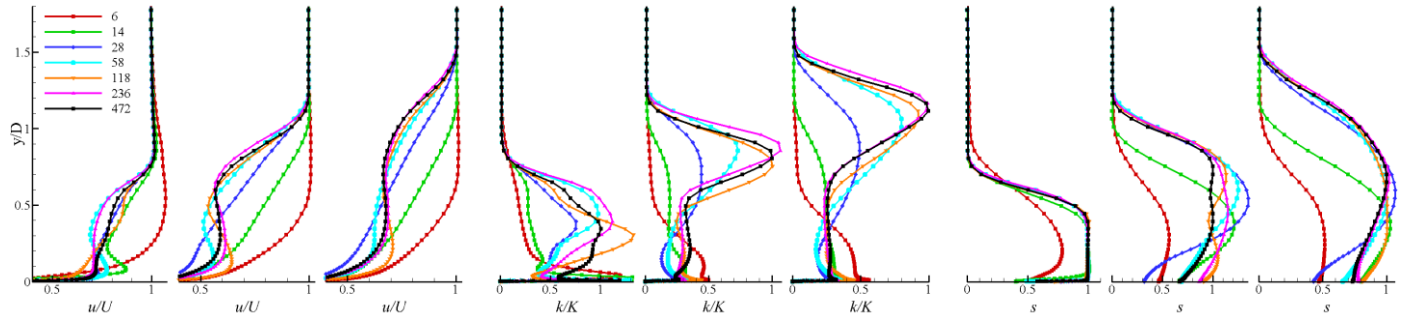

b) M=1.0

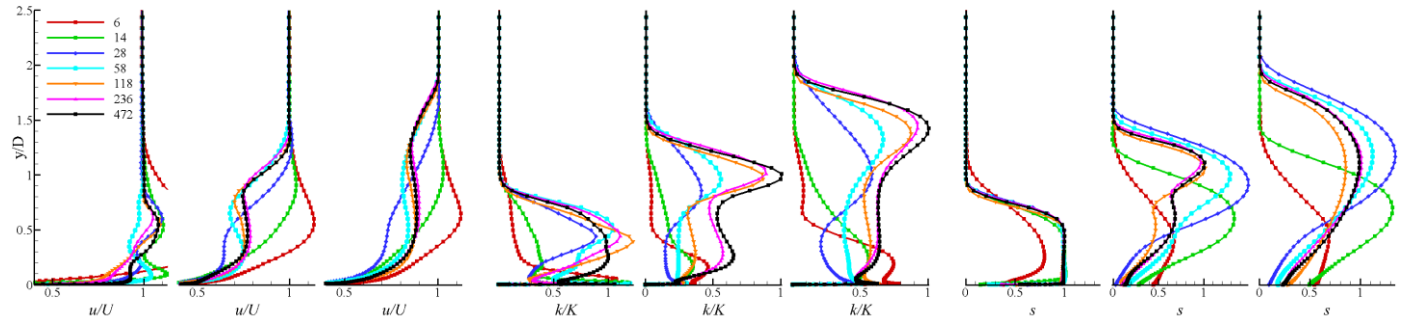

c) M=1.5

Figure A3 Mesh sensitivity of boundary layer profiles with a fixed wall-normal nodes spacing